Published in final edited form as:

Biochemistry. 2017 June 13; 56(23): 2865–2872. doi:10.1021/acs.biochem.7b00241.

Deamidation Slows Curli Amyloid-Protein Aggregation

Hanliu Wang[1,3], **Qin Shu**[2], **Carl Frieden**[2], and **Michael L. Gross**[1,*]

[1]Department of Chemistry, Washington University in St. Louis, St. Louis, MO 63130, United States

[2]Department of Biochemistry and Molecular Biophysics, Washington University School of Medicine, St. Louis, MO 63110, United States

Abstract

Non-enzymatic deamidation of asparagine and glutamine in peptides and proteins is a frequent modification both *in vivo* and *in vitro*. The biological effect is not completely understood, but it is often associated with protein degradation and loss of biological function. Here we describe the deamidation of CsgA, the major protein subunit of curli, which are important proteinaceous components of biofilms. CsgA has a high content of Asn and Gln, a feature seen in a few proteins that self-aggregate. We have implemented an approach to monitor deamidation rapidly by following the globally centroid mass shift, providing guidance for studies at the residue level. From the global mass measurement, we identified, using LC-MS/MS, extensive deamidation of several Asn residues and discovered three “Asn–Gly” sites to be the hottest spots for deamidation. The fibrillization of deamidated CsgA was measured using thioflavin T (ThT) fluorescence, circular dichroism (CD), and a previously reported hydrogen–deuterium exchange (HDX) platform. Deamidated proteins exhibit a longer lag phase and lower final ThT fluorescence, strongly suggesting slower and less amyloid fibril formation. CD spectra show that extensively deamidated CsgA remains unstructured and loses its ability to form amyloids. Mass-spectrometry-based HDX also shows that deamidated CsgA aggregates more slowly than wild-type CsgA. Taken together, the results show that deamidation of CsgA slows its fibrillization and disrupts its function, suggesting an opportunity to modulate CsgA fibrillization and affect curli and biofilm formation.

Graphical Abstract

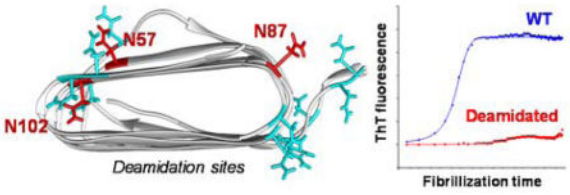

*Corresponding author: Michael L. Gross, Department of Chemistry, Washington University in St. Louis, St. Louis, MO 63130, mgross@wustl.edu.

[3]Current address: Analytical Research and Development, Pfizer Inc., Chesterfield, MO 63017, United States

Supporting Information

The supporting information is available free of charge on the ACS Publications wesite at DOI:

Mechanism of asparagine deamidation; summary of $t_{1/2}$ of the first-order kinetics fit for deamidation.

Keywords

Amyloid fibrillization; deamidation of Asn and Gln; CsgA; biofilm; mass spectrometry; hydrogen deuterium exchange; ThT fluorescence; circular dichroism

Introduction

Biofilms raise concerns in disease, and in medical and industrial settings because they protect bacteria, rendering them resistant to environmental stresses and host defense.[1, 2] The major proteinaceous component of biofilm, curli, are extracellular amyloid fibers that are involved in initial surface adhesion and cell-cell contact in *Escherichia coli*, *Salmonella spp.*, and other enteric bacteria.[3, 4] Aggregation of the major curli subunit CsgA, and factors affecting CsgA aggregation propensities are important because CsgA is a potential target for interrupting biofilm formation.[5, 6] Additionally, this functional amyloid biogenesis may provide hints for understanding disease-associated amyloid formation. Unlike disease-associated amyloid proteins (e.g., Aβ42 in Alzheimer's Disease[7]), functional curli fiber formation is a highly-regulated process.[3, 4] CsgA is secreted as an intrinsically disordered protein (IDP), and rapidly converts to amyloid fibrils at the cell surface. The first 22 residues at the N-terminus are responsible for CsgA outer-membrane secretion, and the rest of sequence is composed of five imperfect, strand-loop-strand repeating units in the fibril.[4] The primary sequence of CsgA has a high content of Asn (16 residues, 12%), Gln (11 residues, 8%), Gly (28 residues, 20%), Ser (12 residues, 9%), and Thr (9 residues, 7%).

Deamidation is commonly associated with reduction or loss of protein function; thus, it may serve as a "Molecular Clock" in biological systems[8]. Enzymatic deamidation only occurs at Gln naturally,[9] for which there is a large interest in the food industry.[10] Free asparagine, not asparagine residues in peptides and proteins, can be deamidated to aspartic acids by asparaginase.[9, 11] Non-enzymatic deamidation of Asn and Gln is widely observed both in vitro and in vivo,[9, 12] and mainly associated with cataract formation and other human aging diseases.[13, 14] As a common process that affects monoclonal-antibody (mAb) function, non-enzymatic deamidation also receives increasing attention in pharmaceutical and biotechnology industries.[13, 15] The half-lives of Asn and Gln deamidation vary extensively, from days to years, depending on the protein and many intrinsic and environmental factors.[8, 9] In general, Asn deamidates faster than Gln.[9] At neutral pH, deamidation of Asn occur via a succinimide intermediate that upon hydrolysis gives Asp and iso-Asp, causing a mass shift of 0.9840 Da (Figure S1).[9, 16] The first-order deamidation rate is largely determined by the primary sequence; residues with low steric hindrance or dipole moments at the carboxyl side of Asn and Gln accelerate deamidation, with Gly causing the largest effect, followed by His and Ser.[8] The deamidation rate is significantly slowed when Asn and Gln residues are involved in secondary and higher-order structures.[9, 12] Temperature, buffer type, pH, and ionic strength also affect protein deamidation rates.[8, 9]

Proteins with rich Asn and Gln regions have high propensity for self-propagating amyloid formation.[17] For example, polyglutamine-containing aggregates may be critical in Huntington's disease.[18] Asn/Gln-rich regions may promote protein–protein interactions,

and, therefore, induce protein aggregation driven by the hydrogen-bond network formed by their polar side chains (also known as “polar zippers”).[17, 19] Deamidation of certain Asn/Gln residues and isomerization of Asp may be linked to several neurodegenerative diseases.[9] Therefore, deamidation is an important, post-translational modification of amyloids. Characterizing deamidation of amyloidal CsgA that contains high content of Asn/Gln could provide a unique perspective for other amyloid proteins.

Mass Spectrometry (MS) is an important tool for characterizing protein deamidation because it has high sensitivity and specificity.[13, 20] Accurate and reliable approaches from chromatographic separation to spectral analysis can overcome problems of co-eluting isomeric products and overlapping isotopic patterns.[13] In this paper, we describe an MS approach to quantify deamidation of amyloid CsgA at the residue level and combine the MS approach with other biophysical approaches to assess the effect of deamidation on CsgA fibrillization.

Materials and Methods

Sample Preparation

CsgA containing a 6xHis-tag at the C-terminus was expressed and purified as previously reported[21], employing a low temperature (~ 4 °C) during purification. Purified CsgA stock was stored at −20 °C in solution containing 6 M guanidine hydrochloride (GdnHCl), 200 mM imidazole, 50 mM potassium phosphate buffer (pH 7.2), and used for deamidation experiments within two weeks of preparation. To follow CsgA deamidation in vitro, CsgA (100 μM) was incubated in a storage buffer at 25 °C or 37 °C for up to 19 days. At various incubation times, a fraction of the sample was buffer exchanged into 50 mM potassium phosphate buffer (pH 7.4) (for CD experiments) or 50 mM potassium phosphate buffer (pH 7.4) containing 150 mM NaCl (for ThT assay) using a Micro Bio-Spin 6 column from BIO-RAD (Hercules, CA) to trigger fibrillization studies.

Materials

D_2O was from Cambridge Isotope Laboratories Inc. (Andover, MA). All other chemicals unless specified were purchased from Sigma–Aldrich (St. Louis, MO).

Analysis of CsgA Deamidation with Mass Spectrometry (MS)

Global-level information of deamidated samples at 25 °C or 37 °C was collected on a Bruker MaXis Q-TOF instrument (Billerica, MA). For each analysis, 5 pmol of CsgA was desalted and eluted from a C8 trap column (Agilent, Santa Clara, CA) in a 3 min linear gradient of 30% – 60% acetonitrile with 0.1% formic acid (FA) at a flow rate of 200 μL/min delivered by a LEAP 3x Ti pump (Carrboro, NC). Molecular weights were obtained with MagTran 1.03.[22] Each global-level experiment was done in duplicate. No degradation of CsgA was observed during incubation.

For residue-level identification and quantification, 1 μL CsgA stock solution at various incubation times was diluted into 50 μL of 2 M urea and 0.1% trifluoroacetic acid, and passed through a custom-packed pepsin column in 1 min. The peptic peptides were trapped

on the C8 column and then eluted with a 5 min linear gradient of 5%–60% acetonitrile (ACN) with 0.1% FA at 50 μL/min. No undigested CsgA was observed under any of these conditions. The eluent was collected, dried in a Savant SpeedVac concentrator SC110 (Thermo Fisher, San Jose, CA), and reconstituted in water with 0.1% FA for auto sampler loading. Approximately 2 pmol of CsgA peptic peptides were loaded onto a 100 μm × 2 cm C18 PepMap RP trapping column (Thermo Fisher, San Jose, CA) and desalted at 5 μL/min for 10 min. Separation was achieved on a 100 μm × 18 cm column custom-packed with 5 μm Magic C18 RP beads (Michrom Bioresources Inc., Auburn, CA) and connected to a stainless steel emitter (Thermo Fisher, San Jose, CA). A gradient was delivered by a nano Ultimate 3000 (Dionex, Co.) at 500 nL/min; 2–32% ACN with 0.1% FA in 44 min, 32–80% ACN with 0.1% FA in 5 min, held at 80% ACN with 0.1% FA for 5 min, returned to 2% ACN in 2 min and re-equilibrated at 2% ACN for 10 min. Mass spectra were collected on a Thermo Q Exactive plus Orbitrap mass spectrometer (San Jose, CA) operated in a data-dependent acquisition mode (to sample the top 15 most abundant ions). Product-ion spectra were submitted to Byonic for identification (Protein Metrics, San Carlos, CA). The search results along with raw files were loaded into Byologic (Protein Metrics, San Carlos, CA) for manual validation and further analysis with their deamidation quantification feature enabled. The deamidation extent was calculated by dividing the areas of peaks (all charge states) representing a deamidation by the sum of all peak areas for the peptide. At each time point, two independent digestions and two injections into the mass spectrometer per sample were employed. Data fitting was performed with one-phase exponential association that is used for the first-order kinetics in Prism 6 (GraphPad, La Jolla, CA).

Thioflavin T (ThT) Assay

Fibrillization of intact (WT) or deamidated CsgA was followed by the change in fluorescence of Thioflavin T (ThT) as previously reported[21] with minor modification. CsgA stock solution was desalted at 100 μM and then diluted to a final concentration of 2 μM in 50 mM potassium phosphate buffer containing 150 mM NaCl and 25 μM ThT (pH 7.4). CsgA of 2 μM instead of 4 μM was used to minimize any stirring and mixing problems caused by heavy aggregates/fibers formed at higher protein concentration. The samples (volume of 1 mL) were incubated at 25 °C with continuous stirring in a glass tube. Change of ThT fluorescence was recorded as a function of time on a spectrofluorometer (Photon Technology International, PTI, Edison, NJ) by using an excitation wavelength of 438 nm and emission at 490 nm.

Circular Dichroism (CD)

Three CsgA samples after zero time (i.e., WT protein, 0 day), 2 days, and 19 days were analyzed by CD to illustrate the effect of deamidation on the secondary structure of CsgA. The samples were buffer exchanged into 50 mM potassium phosphate buffer (pH 7.4) and diluted to 8 μM to start fibrillization. Far-UV CD spectra were recorded on a Jasco-715 spectropolarimeter (Tokyo, Japan) at room temperature as an average of 8 scans from 190 to 260 nm and using a 0.1-cm path cell. The scan rate was 50 nm/min with a response time of 1 s. All samples were manually mixed before taking each reading. The first data point was ~ 12 min after the start of aggregation.

Hydrogen–Deuterium Exchange (HDX)

Pulsed HDX of a 5-day deamidated sample was performed the same way as previously published.[23] Briefly, following buffer exchange, 10 μM deamidated CsgA was incubated at 22 °C and monitored as a function of time by diluting 1:5 into D_2O for 30 s at 4 °C. The HDX was quenched, and protein was subjected to on-line pepsin digestion. The resulting peptic peptides were desalted on a C8 trap column and separated on a 1.9 μm reversed-phase C18 column (Hypersil Gold Thermo Fisher Scientific, Waltham, MA). Data were collected on a Bruker MaXis Q-TOF instrument (Billerica, MA), and analyzed with a custom-developed program implemented in MathCAD (v14, Parametric Technology Corp., MA). Two binomial distributions were used to fit the HDX isotopic envelopes of peptides 26–37, 38–48, and 106–137. The species at high m/z was termed A and that at low m/z B. The fractional species B, which is used to characterize CsgA aggregation propensity, was calculated as $\frac{I_B}{I_A+I_B}$, where I_A and I_B are the MS signal intensities for species A and species B, respectively.

Results and Discussion

Global MS Analysis allows a quick view of CsgA deamidation

The primary sequence of CsgA is prone to deamidation because there is high Asn, Gln, Gly, and Ser content. High concentrations (6–8 M) of guanidine hydrochloride (GdnHCl) are often utilized to prevent CsgA aggregation during purification and storage,[21, 24] which could potentially increase its deamidation rates. To establish an experimental timeframe for following CsgA deamidation at the residue-level, we first employed global-level experiments at 25 and 37 °C. The goal was to obtain information about the time scale of CsgA deamidation in a fast and relatively simple manner to set the stage for residue-level analysis. Therefore, we used a trap column and eluted all forms of CsgA with a short gradient without separation. Because each deamidation site results in 0.9840 Da increase in mass, the isotopic pattern of CsgA continues to shift to higher m/z values as deamidation occurs (Figure 1A), providing a measure of deamidation at the global level. This fast, global-level measurement requires no chromatographic method development and provides guidance for residue-level analysis. We followed the centroid mass shift as a function of time at both 25 °C and 37 °C (Figure 1B). Both datasets fit well with one-phase exponential kinetics, suggesting that CsgA deamidation follows simple first-order kinetics, as expected, at constant pH.

Results of these measurement also show that the deamidation rate is highly temperature-dependent; for example, the mass shift after 19 days of incubation at 25 °C is similar to that of 3-day sample at 37 °C. On the other hand, purified CsgA stored in 6 M GdnHCl at −20 °C showed little to no deamidation for at least 6 months (data not shown). Thus, deamidation can be minimized using low-temperature storage and handling.

Identification and quantification of deamidation by LC–MS/MS

We chose to perform detailed characterization of CsgA deamidation at 37 °C for several time points selected on the basis of global-level information. The commonly used trypsin

digestion in a proteomics experiment is not highly suitable for CsgA because there are only four Arg/Lys out of 137 residues. Three tryptic peptides that contain multiple Asn/Gln are longer than 30 residues, making identification and quantification at the residue-level more difficult than for short peptic peptides. We also avoided trypsin because long enzyme digestion at elevated temperature (i.e., 37 °C) is required, leading to overestimation of the original level of deamidation.[25] We chose pepsin digestion because it is fast and produces multiple overlapping peptides that could increase confidence in data analysis. The result of each residue was determined from the most abundant and short peptide spanning a site. To insure that pepsin digestion was unaffected by deamidation, we checked the result with another peptic peptide (detected with good signal-to-noise ratio) and insured that the results are consistent. The fast on-line digestion and sample handling protocols that are characteristic of pepsin help avoid method artifacts.

Although many of the deamidated peptides can be separated from WT peptides with RP nanoflow HPLC, co-elution does occur, making quantification difficult. Deamidation in the region represented by peptide 38–48 (2+) is an example showing how quantification was carried out using a built-in feature in the Byologic software (Figure 2A). Extracted ion chromatogram (XIC) of the monoisotopic mass 1203.5964 ± 18 ppm of WT is in red (labeled #1). The XIC trace of the monoisotopic mass 1204.5804 ± 18 ppm of the deamidated peptide contains two peaks (#2 in grey and #5 in green). Compared to the isotopic distributions from the tail of peak #1, those from peak #5 suggest a single deamidation site for this peptide (Figure 2B, top and bottom panels). Because peak #5 is well-separated from peak #1, its peak area can be directly used for quantification. The isotopic pattern of the components in the leading edge of peak #2, however, suggests a mixture of WT and deamidated peptides (Figure 2B, middle panel). The theoretical intensity of the first ^{13}C isotope peak from the WT is constructed in Byologic based upon peak #1 (peak #3, red trace at the bottom panel in Figure 2A). Correcting the XIC for the deamidated form represented by the green (peak #4) is accomplished by subtracting the trace of #3 from that of #2. Diagnostic ions b_3, b_4 and the y_4–y_8 series from the MS/MS scans confirm that deamidation occurs at N8 for the substances represented by both peaks #4 and #5 (Figure 2C for peak #4). Because the deamidated and WT peptides coelute as represented by peak #4, the isotopic distributions of daughter ions containing the deamidation site display a mixed pattern, as seen for y_6. It is likely that peak #4 is iso-Asp and #5 is Asp, consistent with the effect on retention time in RP HPLC at low pH.[26] Although electron-capture dissociation or electron-transfer dissociation can further differentiate iso-Asp from Asp,[27, 28] we did not use such but rather combined areas from both peaks to quantify N8 deamidation. A shorter peptic peptide 37–41 shows that less than 1% deamidation occurs at Q3 after 19 days of incubation. This information is not easily revealed by the peptide 38–48 because the two deamidated forms coelute, and there is MS/MS interference from the abundant N8 deamidated peptide. Nevertheless, we are not concerned with quantification of N8 deamidation because the deamidation extent at Q3 is much lower.

We identified a total of fourteen Asn residues showing extensive deamidation (Figure 3). We also observed low deamidation (estimated to be less than 1% even at the longest incubation time) for Gln29, Gln40, Gln74, Asn116, Gln119, and Gln130. Deamidation at Gln is much slower than that of Asn and likely occurs in long-lived proteins in vivo.[9] Contributions from

slow deamidation sites are assumed in this study to be less substantial than those of fast deamidation and, therefore, not included. Peptide 1–25, the most abundant peptide in this region selected for quantification, did not allow deamidation quantification of each Asn residues owing to poor chromatographic separation. Considering that the first 22 residues of CsgA are signal peptides and not as critical as the five repeating units for CsgA aggregation,[4] we summed the results for the first four Asn residues. Deamidation at Asn124/125 was also quantified as one group because co-elution did not allow further resolution. All the residue-level data were fit with the first-order kinetics (Figure 3A), as obtained at the global-level. A list of $t_{1/2}$ values extracted from each fit is provided in Table S1. Among the eight Asn residues that were quantified at the residue level, the $t_{1/2}$ values for Asn 57, 87, and 102 are significantly shorter than for Asn 34, 45, 79, 90, and 112 at 95% confidence. Mapping these residues onto the primary sequence of CsgA (Figure 3B) makes it clear that the differences in deamidation kinetics are caused by the residues on the carboxyl side of Asn. Asn 57, 87, and 102 are the only three residues followed by Gly, a combination that is known to be the "hot spot" for deamidation owing to minimal steric effects.[9] Asn 34, 45, 79, 90, and 112 are followed by a polar residue Ser that can enhance deamidation by stabilizing the succinimide intermediate.[9] The primary sequence of CsgA seems to be the major determinant for fast deamidation. These hot spots for deamidation are conserved in CsgA from different enteric bacteria. It is interesting to ask why CsgA would employ such an unstable primary sequence when its role is to form highly controlled amyloid fibrils.

Thioflavin T (ThT) Assay

Because thioflavin T(ThT) fluorescence increases upon binding to β-sheet-rich surfaces, it is frequently used to follow amyloid fibril formation *in vitro*.[29, 30] Given that curli are functional amyloids that share many of the biophysical properties of disease-associated amyloids, curli and its major protein subunit CsgA, once fibrillated, can bind ThT.[31] Thus, the ThT assay was widely used in monitoring the aggregation/fibrillization of CsgA in vitro.[5, 21, 24, 32–34] To examine the effect of deamidation on the biological function of CsgA, we followed the kinetic change of ThT fluorescence during the aggregation/fibrillization of CsgA. We note that the lag phase here for intact CsgA (Figure 4A, 0 d) is shorter than that reported previously[5, 21, 24], possibly because the concentration after desalting was initially 100 μM before diluted to 2 μM for the ThT assay. Nevertheless, comparison of fibrillization (aggregation) beween WT and deamided CsgA is not affected. The outcomes are sigmoidal curves in ThT fluorescence as for the WT over 10 days but with different lag phases and plateaus (Figure 4A). CsgA that is more deamidated shows longer lag phases and less ThT fluorescence, indicating slower and less extensive fibril formation. Moreover, CsgA deamidated for 19 days shows little or no ThT fluorescence, indicating an inability to form β-sheet fibrils. These results clearly show that deamidation of CsgA slows the rate and lowers the concentration of ThT-positive aggregates/fibers.

Circular Dichroism (CD) Analysis

To understand the general structural features of the deamidated CsgA, we compared, using CD, the secondary structural changes of WT and deamidated CsgA after 2 and 19 days of incubation. The WT CsgA shows a time-dependent structural change with a decrease in

disordered random coil (minimum at ~ 200 nm) and an increase in ordered structure (minimum at ~ 220 nm), indicating aggregation and a transition from disordered random coil to ordered fiber with β-sheet structure (Figure 5A). In contrast, CsgA deamidated for 2 days shows a less ordered structure and a slower decrease of disordered structure (Figure 5B). As shown in Figure 5D, the kinetics of protein aggregation, as monitored by CD at 200 nm after deamidation for 2 days compared to no deamidation were fitted to a single-exponential function; the rate constants are 0.019 ± 0.004 and 0.044 ± 0.005 h^{-1}, respectively. Essentially no change was observed for the protein deamidated for 19 days. CsgA deamidated for 2 days undergoes structural change ~2-fold slower than WT (Figure 5D), whereas CsgA deamidated for 19 days shows no further change and maintains its disordered structure (Figure 5C). Deamidated CsgA, after 2 days still can form aggregates/fibers as shown by binding to ThT.

Hydrogen–Deuterium Exchange (HDX)

We previously applied HDX to study conformation and to follow the aggregation of curli proteins.[23, 35] In an application to CsgA, we discovered two species with distinct deuterium labeling extents during aggregation. Species A at higher *m/z* exchanges rapidly, similar to that of a denatured monomer, whereas species B at lower *m/z* is structured and well-protected.[23] The abundance of species B relative to that of A reflects aggregation propensities and is used to follow the aggregation at the peptide-level.

We utilized the same HDX protocol to study aggregation of CsgA deamidated for 5 days and compared the results to those of the WT[23]. The HDX of the deamidated and WT CsgA at the beginning of aggregation are similar because both forms are highly dynamic, disordered, and solvent exposed. The buildup of species B, however, is much slower for the deamidated CsgA than for the WT (Figure 6), indicating that the deamidated protein loses its ability to form fibrils. For the times used here, we only observed slight increases in the fraction B species for the three peptides 26–37, 38–48, and 106–137 representing R1 and R5, which also show faster aggregation for the WT.[23]

Effect of Deamidation on Curli Fibril Formation

Our results from ThT fluorescence, CD, and HDX taken together indicate that deamidated CsgA loses its ability to form fibrils (i.e., deamidation decreases its aggregation propensity). Although the mechanism of aggregation is unclear, it is often positively correlated with deamidation propensity (i.e., deamidation increases the aggregation propensity), possibly owing to decreased stability and altered structures.[14, 15, 26] Although aggregation is used often as a general term, here it refers to controlled fibrillization that fulfills the natural function of CsgA, and it is negatively correlated with deamidation. These two seemingly contrasting views on the relationship of deamidation and protein aggregation may arise from the different mechanisms of protein aggregation. Nevertheless, all studies of deamidation and aggregation demonstrate that deamidation leads to a loss of protein function.

We mapped the extensive deamidated Asn residues onto a predicted left-handed CsgA structure[36] in the fibril (Figure 7). The three fastest deamidation sites are colored in red, and the remaining Asn residues are in cyan. All the deamidation sites are located at or near the

loop-turn regions of the structure, and most point outwards from the amyloid core. That CsgA fibrillization is significantly slowed after 1 and 2 days of deamidation is consistent with the large effect caused by the three fast deamidating residues, Asn57, 87, and 102, despite their location in the less amyloidogenic repeating units R2, R3, and R4.[23, 24] There are at least three explanations why deamidated CsgA forms fibers much more slowly. The first is that Asn, which is critical for CsgA amyloid formation, and Gln form hydrogen bonds with the nearby protein backbone and thereby increase the stability of the β-sheet of the amyloid fibril.[19, 37] The resultant Asp and Glu, from deamidation of Asn and Gln, do not have this advantage. Second, the effect introduced by the negative charge of Asp or iso-Asp, made available as a result of deamidation, slows fibrillization by Coulomb repulsion. One of the strategies employed by proteins to avoid edge-to-edge aggregation between β-sheets is inward-pointing charges.[38] Development of charge cannot be the sole reason because this effect loses importance for other proteins where deamidation increases aggregation. Third, function is lost because formation of the iso-Asp product introduces an additional β-carbon into protein backbone and thereby significantly alters its structure and function.[39–41] Although iso-Asp may be favored over Asp in the hydrolysis of succinimide intermediate,[16] it is difficult to differentiate iso-Asp from Asp with MS-based collision-induced dissociation (CID). Thus, we cannot attribute any specific effect from iso-Asp.

Wang et al[32] showed that Ala substitutions of eight internally conserved Gln's and five Asn's increase SDS solubility of curli, suggesting that these polar residues help stabilize the amyloids. However, Ala substitution of only four residues, Gln29, Asn34, Gln119, and Asn124, impedes CsgA fibrillization in vivo and in vitro.[32] None of these residues are identified as the fast deamidation site in this work. Loss of Asn is unlikely to be the most important factor here. It was also found that several Asp and Gly residues are "gatekeepers".[42] Substitutions of the four Asp's with two Leu, one Asn, and one His, along with three Gly substitutions, result in faster CsgA aggregation. DePace et al[43] reported that substitutions of Gln and Asn, to mainly positively charged residues, lead to increased solubility of prion protein Sup35p, or even cause curing of amyloids in vivo. Both suggest the significant impact of charged residues on amyloid proteins. Therefore, the negative charges introduced by the iso-Asp or Asp are likely important in preventing CsgA amyloid formation. As stated above, however, charging of the protein cannot be the only factor. This hypothesis can be tested in the future with mutagenesis studies.

Conclusion

Understanding the functional amyloid CsgA, the major curli component, may be a useful reference for disease-associated, uncontrolled amyloid formation. Here we show that CsgA fibrillization and biofilm formation become slower upon deamidation.[5, 6] The global-level results show that CsgA deamidation in a storage buffer is temperature dependent and obeys one-phase, first-order kinetics. We found extensive deamidation of 14 Asn residues in CsgA, particularly at three hot spots comprised of "Asn–Gly". The primary sequence of CsgA is highly susceptible to deamidation because most Asn residues adjoin other residues that enhance deamidation rates.[8, 9] ThT fluoresence assays show fibers form more slowly when CsgA is deamidated under stress. WT CsgA forms a highly organized β-sheet whereas deamidated CsgA remains unstructured as observed by both CD and HDX studies. Site-

directed mutagenesis in the future will pinpoint the critical Asn residues among candidates identified in this work. Purposeful and controlled deamidation might be used as an approach to modulate CsgA fibrillization. For example, adding a synthetic "asparaginase" can accelerate deamidation rates of "Asn–Gly"[44] and may significantly disrupt curli fiber formation.

Supplementary Material

Refer to Web version on PubMed Central for supplementary material.

Acknowledgments

We thank Dr. Chris Becker from Protein Metrics for his help with the deamidation quantification feature in Byologics. This work was supported by NIH National Institutes of General Medical Sciences: 2P41GM103422 to M.L.G and 1R01AI099099 to C.F. Instrumentation was provided by the NIH 1S10OD016298.

References

1. Hall-Stoodley L, Costerton JW, Stoodley P. Bacterial biofilms: from the natural environment to infectious diseases. Nat Rev Microbiol. 2004; 2:95–108. [PubMed: 15040259]
2. Hall-Stoodley L, Stoodley P. Evolving concepts in biofilm infections. Cell Microbiol. 2009; 11:1034–1043. [PubMed: 19374653]
3. Evans ML, Chapman MR. Curli biogenesis: order out of disorder. Biochim Biophys Acta. 2014; 1843:1551–1558. [PubMed: 24080089]
4. Barnhart MM, Chapman MR. Curli biogenesis and function. Annu Rev Microbiol. 2006; 60:131–147. [PubMed: 16704339]
5. Cegelski L, Pinkner JS, Hammer ND, Cusumano CK, Hung CS, Chorell E, Aberg V, Walker JN, Seed PC, Almqvist F, Chapman MR, Hultgren SJ. Small-molecule inhibitors target Escherichia coli amyloid biogenesis and biofilm formation. Nat Chem Biol. 2009; 5:913–919. [PubMed: 19915538]
6. Cegelski L, Marshall GR, Eldridge GR, Hultgren SJ. The biology and future prospects of antivirulence therapies. Nat Rev Microbiol. 2008; 6:17–27. [PubMed: 18079741]
7. Giacobini E, Gold G. Alzheimer disease therapy--moving from amyloid-beta to tau. Nat Rev Neurol. 2013; 9:677–686. [PubMed: 24217510]
8. Robinson NE, Robinson AB. Molecular clocks. Proc Natl Acad Sci U S A. 2001; 98:944–949. [PubMed: 11158575]
9. Robinson, NE., Robinson, AB. Molecular clocks: deamidation of asparaginyl and glutaminyl residues in peptides and proteins. Althouse Press; Cave Junction, OR: 2004.
10. Gaspar AL, de Goes-Favoni SP. Action of microbial transglutaminase (MTGase) in the modification of food proteins: a review. Food Chem. 2015; 171:315–322. [PubMed: 25308675]
11. Batool T, Makky EA, Jalal M, Yusoff MM. A comprehensive review on L-asparaginase and its applications. Appl Biochem Biotechnol. 2016; 178:900–923. [PubMed: 26547852]
12. Robinson NE. Protein deamidation. Proc Natl Acad Sci U S A. 2002; 99:5283–5288. [PubMed: 11959979]
13. Hao P, Adav SS, Gallart-Palau X, Sze SK. Recent advances in mass spectrometric analysis of protein deamidation. Mass Spectrom Rev. 2016; doi: 10.1002/mas.21491
14. Lampi KJ, Wilmarth PA, Murray MR, David LL. Lens beta-crystallins: the role of deamidation and related modifications in aging and cataract. Prog Biophys Mol Biol. 2014; 115:21–31. [PubMed: 24613629]
15. Gervais D. Protein deamidation in biopharmaceutical manufacture: understanding, control and impact. Journal of Chemical Technology and Biotechnology. 2016; 91:569–575.

16. Capasso S, Di Cerbo P. Kinetic and thermodynamic control of the relative yield of the deamidation of asparagine and isomerization of aspartic acid residues. J Pept Res. 2000; 56:382–387. [PubMed: 11152297]
17. Michelitsch MD, Weissman JS. A census of glutamine/asparagine-rich regions: implications for their conserved function and the prediction of novel prions. Proc Natl Acad Sci U S A. 2000; 97:11910–11915. [PubMed: 11050225]
18. Hoffner G, Djian P. Polyglutamine aggregation in huntington disease: does structure determine toxicity? Mol Neurobiol. 2015; 52:1297–1314. [PubMed: 25336039]
19. Perutz MF, Johnson T, Suzuki M, Finch JT. Glutamine repeats as polar zippers: their possible role in inherited neurodegenerative diseases. Proc Natl Acad Sci U S A. 1994; 91:5355–5358. [PubMed: 8202492]
20. Jha SK, Deepalakshmi PD, Udgaonkar JB. Characterization of deamidation of barstar using electrospray ionization quadrupole time-of-flight mass spectrometry, which stabilizes an equilibrium unfolding intermediate. Protein Sci. 2012; 21:633–646. [PubMed: 22431291]
21. Shu Q, Crick SL, Pinkner JS, Ford B, Hultgren SJ, Frieden C. The E. coli CsgB nucleator of curli assembles to beta-sheet oligomers that alter the CsgA fibrillization mechanism. Proc Natl Acad Sci U S A. 2012; 109:6502–6507. [PubMed: 22493266]
22. Zhang Z, Marshall AG. A universal algorithm for fast and automated charge state deconvolution of electrospray mass-to-charge ratio spectra. J Am Soc Mass Spectrom. 1998; 9:225–233. [PubMed: 9879360]
23. Wang H, Shu Q, Rempel DL, Frieden C, Gross ML. Understanding curli amyloid-protein aggregation by hydrogen–deuterium exchange and mass spectrometry. Int J Mass Spectrom. 2016; doi: 10.1016/j.ijms.2016.10.006
24. Wang X, Smith DR, Jones JW, Chapman MR. In vitro polymerization of a functional Escherichia coli amyloid protein. J Biol Chem. 2007; 282:3713–3719. [PubMed: 17164238]
25. Du Y, Wang F, May K, Xu W, Liu H. Determination of deamidation artifacts introduced by sample preparation using 18O-labeling and tandem mass spectrometry analysis. Anal Chem. 2012; 84:6355–6360. [PubMed: 22881398]
26. Nilsson MR, Driscoll M, Raleigh DP. Low levels of asparagine deamidation can have a dramatic effect on aggregation of amyloidogenic peptides: implications for the study of amyloid formation. Protein Sci. 2002; 11:342–349. [PubMed: 11790844]
27. Cournoyer JJ, Pittman JL, Ivleva VB, Fallows E, Waskell L, Costello CE, O'Connor PB. Deamidation: differentiation of aspartyl from isoaspartyl products in peptides by electron capture dissociation. Protein Sci. 2005; 14:452–463. [PubMed: 15659375]
28. Ni W, Dai S, Karger BL, Zhou ZS. Analysis of isoaspartic Acid by selective proteolysis with Asp-N and electron transfer dissociation mass spectrometry. Anal Chem. 2010; 82:7485–7491. [PubMed: 20712325]
29. Vassar PS, Culling CF. Fluorescent stains, with special reference to amyloid and connective tissues. Arch Pathol. 1959; 68:487–498. [PubMed: 13841452]
30. Biancalana M, Koide S. Molecular mechanism of Thioflavin-T binding to amyloid fibrils. Biochim Biophys Acta. 2010; 1804:1405–1412. [PubMed: 20399286]
31. Chapman MR, Robinson LS, Pinkner JS, Roth R, Heuser J, Hammar M, Normark S, Hultgren SJ. Role of Escherichia coli curli operons in directing amyloid fiber formation. Science. 2002; 295:851–855. [PubMed: 11823641]
32. Wang X, Chapman MR. Sequence determinants of bacterial amyloid formation. J Mol Biol. 2008; 380:570–580. [PubMed: 18565345]
33. Wang X, Hammer ND, Chapman MR. The molecular basis of functional bacterial amyloid polymerization and nucleation. J Biol Chem. 2008; 283:21530–21539. [PubMed: 18508760]
34. Andersson EK, Bengtsson C, Evans ML, Chorell E, Sellstedt M, Lindgren AE, Hufnagel DA, Bhattacharya M, Tessier PM, Wittung-Stafshede P, Almqvist F, Chapman MR. Modulation of curli assembly and pellicle biofilm formation by chemical and protein chaperones. Chem Biol. 2013; 20:1245–1254. [PubMed: 24035282]

35. Wang H, Shu Q, Rempel DL, Frieden C, Gross ML. Continuous and pulsed hydrogen–deuterium exchange and mass spectrometry characterize CsgE oligomerization. Biochemistry. 2015; 54:6475–6481. [PubMed: 26418947]

36. Tian P, Boomsma W, Wang Y, Otzen DE, Jensen MH, Lindorff-Larsen K. Structure of a functional amyloid protein subunit computed using sequence variation. J Am Chem Soc. 2015; 137:22–25. [PubMed: 25415595]

37. Srinivasan N, Anuradha VS, Ramakrishnan C, Sowdhamini R, Balaram P. Conformational characteristics of asparaginyl residues in proteins. Int J Pept Protein Res. 1994; 44:112–122. [PubMed: 7982754]

38. Richardson JS, Richardson DC. Natural beta-sheet proteins use negative design to avoid edge-to-edge aggregation. Proc Natl Acad Sci U S A. 2002; 99:2754–2759. [PubMed: 11880627]

39. Doyle HA, Mamula MJ. Post-translational protein modifications in antigen recognition and autoimmunity. Trends Immunol. 2001; 22:443–449. [PubMed: 11473834]

40. Noguchi S. Structural changes induced by the deamidation and isomerization of asparagine revealed by the crystal structure of Ustilago sphaerogena ribonuclease U2B. Biopolymers. 2010; 93:1003–1010. [PubMed: 20623666]

41. Moss CX, Matthews SP, Lamont DJ, Watts C. Asparagine deamidation perturbs antigen presentation on class II major histocompatibility complex molecules. J Biol Chem. 2005; 280:18498–18503. [PubMed: 15749706]

42. Wang X, Zhou Y, Ren JJ, Hammer ND, Chapman MR. Gatekeeper residues in the major curlin subunit modulate bacterial amyloid fiber biogenesis. Proc Natl Acad Sci U S A. 2010; 107:163–168. [PubMed: 19966296]

43. DePace AH, Santoso A, Hillner P, Weissman JS. A critical role for amino-terminal glutamine/asparagine repeats in the formation and propagation of a yeast prion. Cell. 1998; 93:1241–1252. [PubMed: 9657156]

44. Gibbs RA, Taylor S, Benkovic SJ. Antibody-catalyzed rearrangement of the peptide bond. Science. 1992; 258:803–805. [PubMed: 1439788]

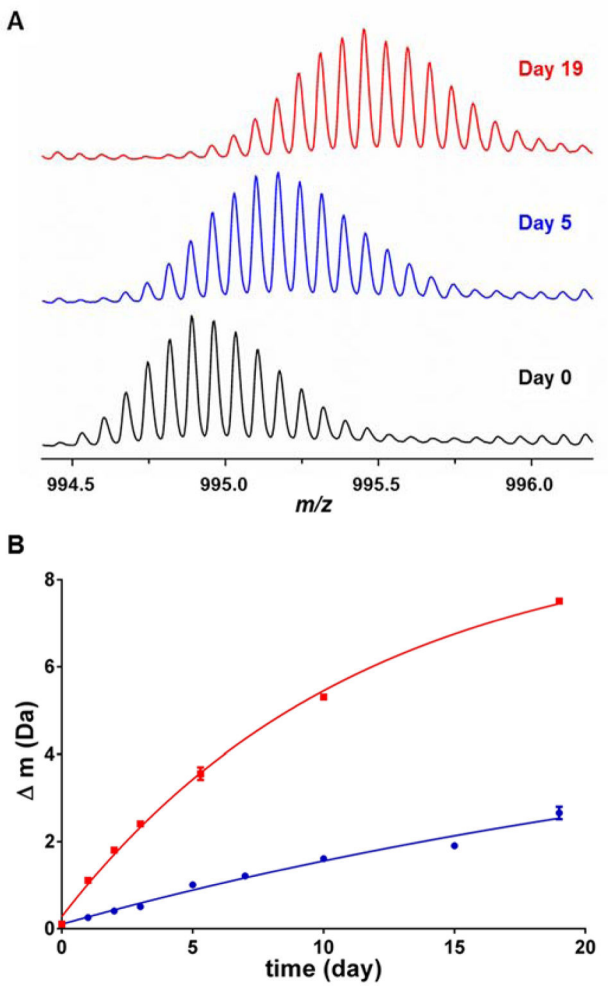

Figure 1.

Deamidation of CsgA monitored for the intact protein (global analysis). (A) Isotopic distributions of charge state 14 at day 0 (black), day 5 (blue), and day 19 (red) at 37 °C. (B) Centroid mass shift of deamidated CsgA compared to that of WT as a function of different deamidation times at 25 °C (blue) and 37 °C (red). Data were fit with first-order kinetics

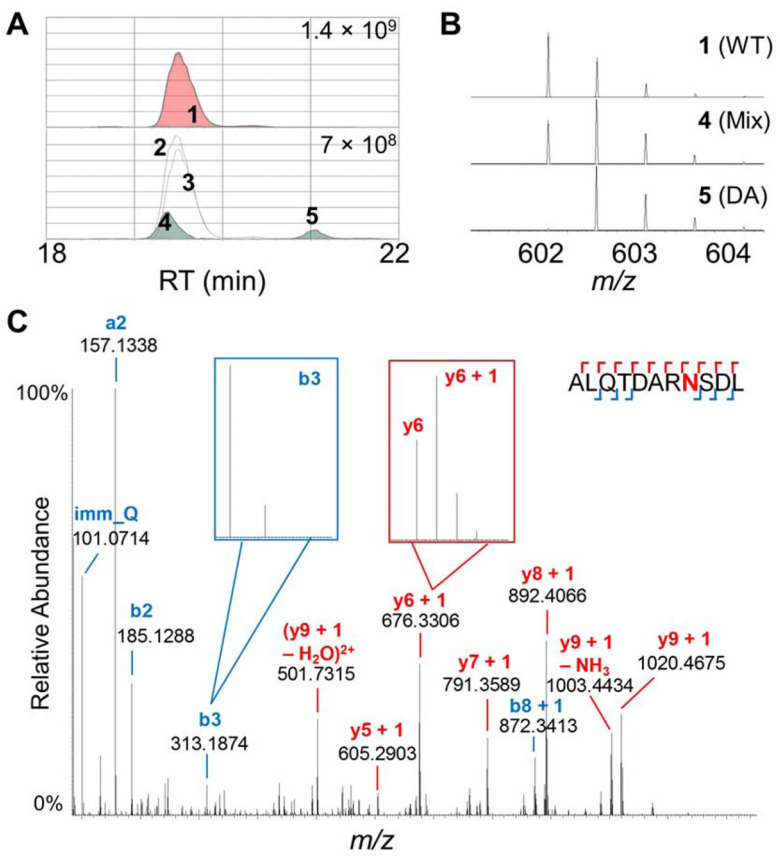

Figure 2.

(A) Extracted ion chromatogram of WT (top) and deamidated form (bottom) peptide 38–48. (B) isotopic distributions at peak #1 (WT), 4 (mix of WT and deamidated form), and 5 (deamidated form). (C) Product-ion (MS/MS) spectrum of components represented by peak #4 (mix of WT and deamidated form). Isotopic patterns of b_3 and y_6 are zoomed in. Major peaks are annotated. All identified b and y ions are marked on the peptide sequence, and the deamidation site highlighted in red

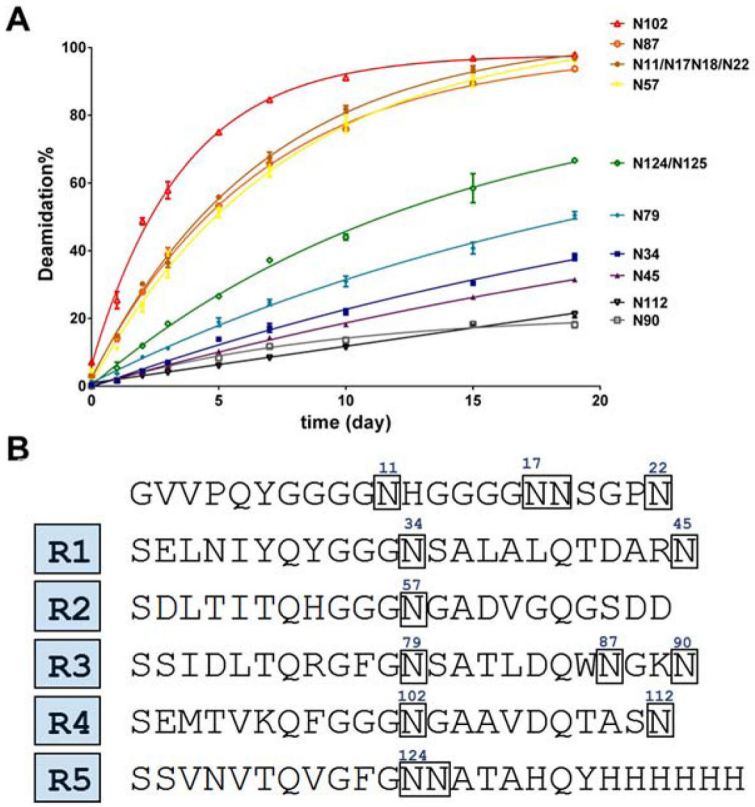

Figure 3.

(A) Quantification of CsgA deamidation at the residue level. All data were fit with first-order kinetics. Identified residues are labeled on the right. (B) Deamidated residues mapped onto the primary sequence of CsgA.

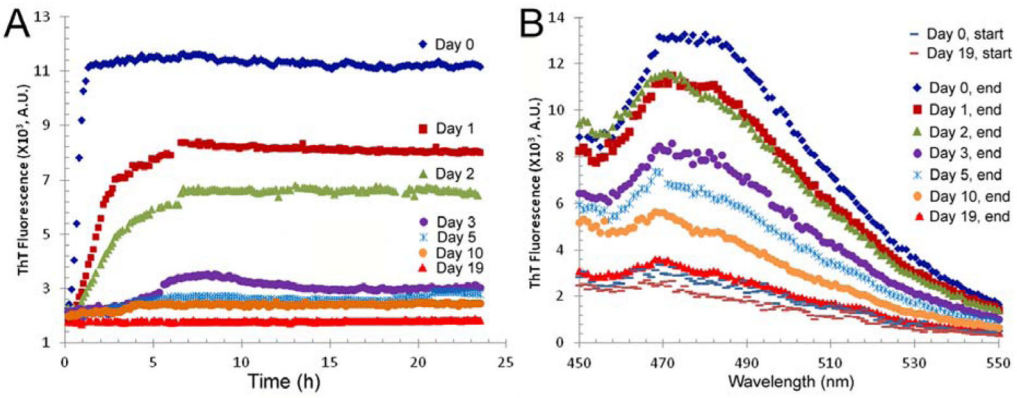

Figure 4.

Fibrillization of intact and deamidated CsgA as monitored by Thioflavin T (ThT) fluorescence. (A) Time course of ThT fluorescence change. (B) Emission scan of different deaminated CsgA at the plateau phase (~24 h) of ThT assay.

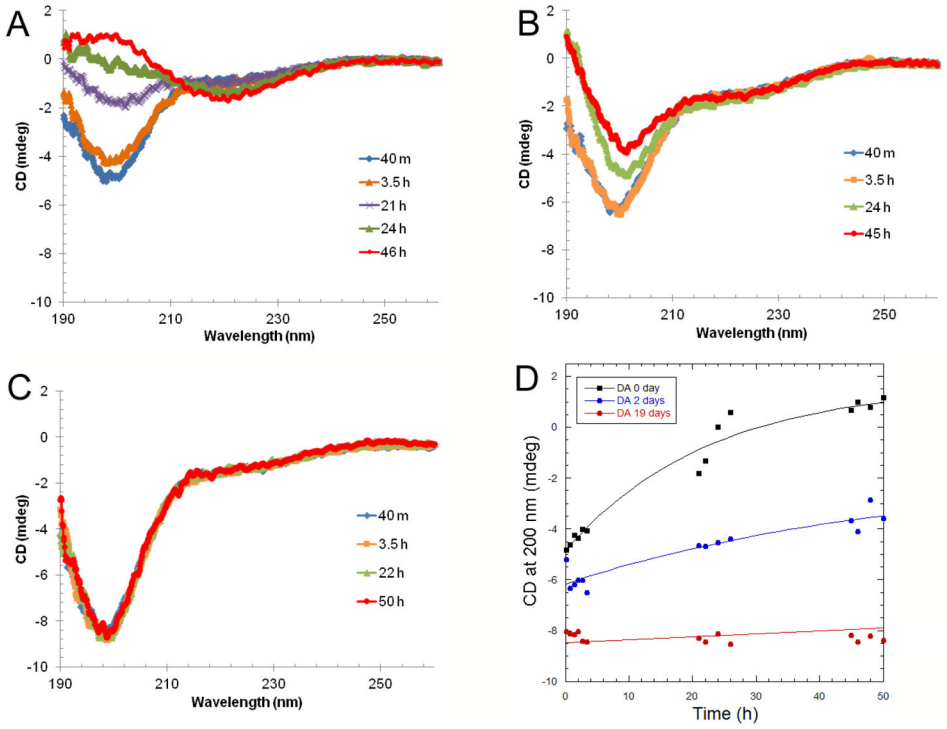

Figure 5.

Aggregation of CsgA as monitored by far-UV CD. CD spectra of (A) Intact CsgA (DA 0 day) (B) CsgA deamidated 2 days (DA 2 days) and (C) deamidated 19 days (DA 19 days) at different incubation times (figure legend). (D) Kinetic change of disordered structure of different CsgA sample as shown by CD at 200 nm.

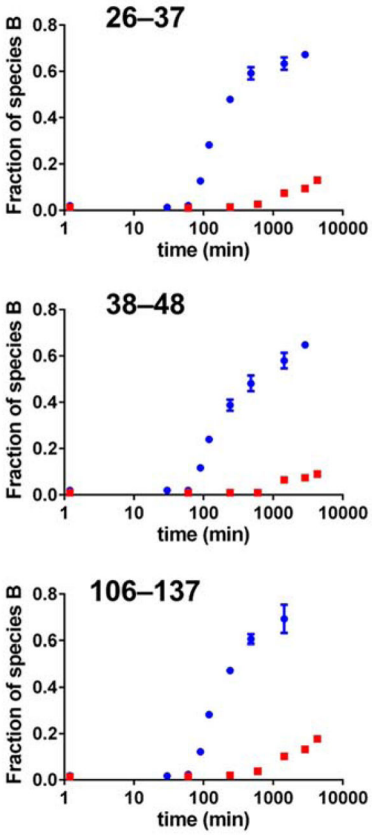

Figure 6.

Fraction species B of WT (blue) and deamidated (red) as a function of incubation time for peptides 26–37, 38–48, and 106–137.

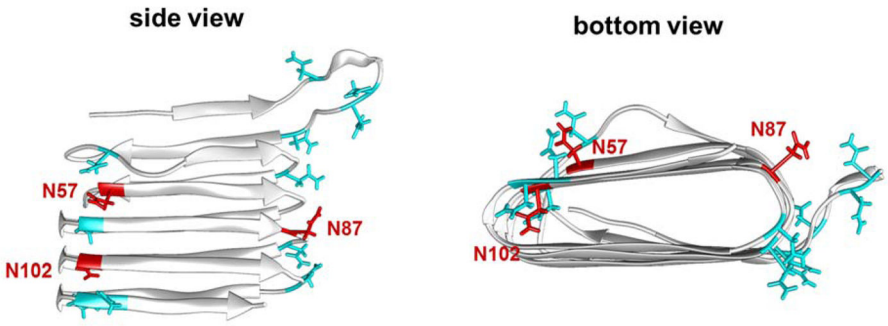

Figure 7.

Deamidated residues mapped onto a predicted CsgA structure[36] in fibrils. The three fast deamidation sites are labeled and colored in red.